# Regulation of tillering in sorghum: environmental effects

**Hae Koo Kim[1,2,†], Erik van Oosterom[1], Michael Dingkuhn[2], Delphine Luquet[2] and Graeme Hammer[1,*]**

[1]*The University of Queensland, School of Land, Crop and Food Sciences, Brisbane, QLD 4072, Australia and* [2]*CIRAD, UPR 59, Avenue Agropolis Lavalette TA A 59/01, 34398 Montpellier, France*

*\* For correspondence. E-mail g.hammer@uq.edu.au*

†*Current address: Pohang University of Science and Technology, Biofluid and Biomimic Research Center, San 31, Hyoja Dong, Namgu, Pohang, 790-784, South Korea.*

• *Background and Aims* Tillering has a significant effect on canopy development and, hence, on resource capture, crop growth and grain yield in sorghum. However, the physiological basis of tillering and its regulation by environmental effects are not fully understood. The objective of this study was to understand and quantify the environmental effects on tillering in sorghum using a carbohydrate supply–demand framework.

• *Methods* A series of five experiments with a wide range of radiation and temperature conditions was conducted and details of the tillering responses of a single representative hybrid were monitored. The concept of internal plant competition for carbohydrate was developed for analysis of these responses.

• *Key Results* Tiller appearance was highly synchronized with main shoot leaf appearance, with a consistent hierarchy for tillering across environments. The main environmental effect was on the frequency of tiller appearance, in particular of the lower-rank tillers. This explained some of the observed environmental differences in the onset of tillering. A generalized index of internal plant competition, which took account of plant assimilate supply and demand ($S/D_{index}$) during the critical period for tillering, explained most of the variation in maximum tiller number observed across the five experiments.

• *Conclusions* This result was consistent with the hypothesis that internal plant competition for assimilates regulates tillering in sorghum. Hence, the framework outlined has a predictive value that could provide the basis for dynamic simulation of tillering in crop growth models.

**Key words:** Carbohydrate supply–demand ratio, internal plant competition, leaf area development, modelling, radiation, *Sorghum bicolor*, temperature, tiller hierarchy.

## INTRODUCTION

Tillering is an important agronomic trait in many high-tillering cereals such as wheat (*Triticum aestivum*), rice (*Oryza sativa*) and barley (*Hordeum vulgare*), and contributed significantly to improved yield associated with the 'green revolution' (Conway and Toenniessen, 1999; Khush, 1999). Although tillering is considerably less in sorghum (*Sorghum bicolor*), it nonetheless has a major influence on plant leaf area development (Hammer *et al.*, 1987; Lafarge *et al.*, 2002) and, hence, on crop water-use patterns and adaptation to water-limited environments (van Oosterom *et al.*, 2008). Modern sorghum hybrids produce from zero to four fertile tillers in field conditions so that at plant densities below $4\ m^{-2}$, around 70–80 % of total plant leaf area and grain yield can be attributed to tillers (Lafarge *et al.*, 2002; Lafarge and Hammer, 2002*b*).

The ecophysiological basis of tillering and its regulation by environmental and genetic effects are not fully understood. Hence, its formalization in most crop models is limited. In sorghum, early attempts at modelling were based on concepts considering tillers as similar to the main shoot (Heiniger *et al.*, 1997; Rosenthal *et al.*, 1989). Later attempts allowed for differences in size among main shoot and tillers (Hammer *et al.*, 1993; Hammer and Muchow, 1994), but remained

descriptive and still required input of tiller number. In related, but higher tillering species, such as pearl millet (*Pennisetum glaucum*), differences in number and size of leaves on individual tillers have been included in crop models. Although this allowed simulation of genotypic differences in fertile tiller number via effects on inter-axis competition, the number of emerged tillers remained an input to the model (van Oosterom *et al.*, 2001).

Studies on tiller number dynamics in rice, wheat, barley and ryegrass (*Lolium perenne*) have used the concept of site filling (Katayama, 1951; Davies and Thomas, 1983; Neuteboom and Lantinga, 1989). Potential tillering sites formed in a fixed pattern with a definite regularity and interval in relation to main shoot development, with a tiller bud produced at the base of every leaf (Bos and Neuteboom, 1998; Kirby *et al.*, 1985). Realized tiller number was then determined by the number of these buds that grew out into tillers (Li *et al.*, 2003). The fraction of buds that ultimately developed into a productive tiller at a specific site has been associated with a number of factors. Studies on wheat (Friend, 1965), rice (Honda and Okajima, 1970), barley (Kirby and Faris, 1972) and ryegrass (Ong and Marshall, 1979) have suggested that tiller outgrowth depended on resource availability (nitrogen and carbohydrate) for the crop, but this was not pursued to

quantification at the individual plant level. Lafarge and Hammer (2002*b*) detailed how plant internal competition for carbohydrate could be applied to modelling dynamics of tiller fertility in sorghum. Dingkuhn *et al.* (2006) and Luquet *et al.* (2006) applied this concept to model rice morphogenesis based on the ratio between carbohydrate supply and demand (*S/D*). In these studies, *S/D* was shown to be a key factor controlling tiller emergence, growth and survival. Tillering is also known to be controlled by light quality via the red/far-red ratio (Deregibus *et al.*, 1985; Casal *et al.*, 1986; Evers *et al.*, 2006), but studies in sorghum have suggested that this probably relates to timing of cessation of tiller outgrowth due to plant-to-plant competition, rather than to initiation of tiller outgrowth associated with internal plant competition (Lafarge and Hammer, 2002*b*).

The *S/D* ratio is a complex indicator of plant carbohydrate status that depends on both environmental and genotypic factors. Solar radiation and temperature are the main environmental factors that affect *S/D*. Radiation is a key regulator of photosynthesis and hence of plant carbohydrate supply and growth (Johnson *et al.*, 1995; Choudhury, 2001). In contrast, temperature has a major influence on developmental processes such as node and leaf production and expansion rates, which affect crop leaf area index (LAI) and hence carbohydrate demand (Hammer *et al.*, 1993; Tardieu *et al.*, 1999; Mazzella *et al.*, 2000). The ratio of these two key environmental factors was defined by Nix (1976) as the photo-thermal quotient (PTQ, MJ m$^{-2}$ $^{\circ}$Cd$^{-1}$) and has been commonly used as an environmental indicator of carbohydrate availability for plant growth. A high PTQ indicates that more carbohydrate can be produced per developmental unit and suggests an excess of supply over demand. This concept has been used in quantifying environmental effects on grain number in cereals (Fischer and Wilson, 1975; Ortiz-Monasterio *et al.*, 1994). However, it does not include the fraction of incoming radiation that is intercepted by plants, which is critically dependent on leaf area development in the early stages of the crop cycle (Lafarge and Hammer, 2002*a*). In the first few weeks after emergence until panicle initiation, main shoot leaf area is both the unique supplier and the main sink for carbohydrates, and total plant leaf area dynamics can be directly linked to tiller production (Hammer *et al.*, 1987).

In sorghum, the environmental and genotypic control of tillering has not been addressed comprehensively using the carbohydrate *S/D* framework. Although Lafarge *et al.* (2002) used this framework to describe a hierarchy for tiller emergence and fertility across a range of densities in a single environment for a specific genotype, detailed physiological studies on tillering across a range of environments and genotypes have not been reported.

The objective of this study was to better understand and quantify the environmental effects regulating tillering in sorghum. It was hypothesized that these effects operated via their influences on internal plant competition for carbohydrate. A series of five experiments, which generated contrasting levels of plant internal competition for carbohydrates by imposing a wide range of photo-thermal conditions, was used to explore tillering responses of one representative hybrid. Genetic effects are addressed in a companion study (Kim *et al.*, 2010).

## MATERIALS AND METHODS

### Experimental details

A high-tillering, well-adapted Australian sorghum (*Sorghum bicolor* L. Moench) hybrid ['Midge Resistant (MR) Buster'] was grown in five experiments (three field experiments and two controlled environment experiments) that generated a wide range in plant *S/D* levels (Table 1).

The field experiments were conducted over two summer seasons. Experiment 1 (expt 1) was sown on 25 October, 2004 at Warwick (28 $^{\circ}$12′S, 152 $^{\circ}$5′E, elevation 462 m asl) in the sorghum belt of eastern Australia. The early sowing date resulted in relatively low maximum temperature, but high radiation levels (Table 1). Experiment 2 (expt 2) was sown at Warwick on 2 March, 2005 during late summer, but experienced similar temperature and radiation as expt 1. Experiment 3 (expt 3) was sown at Gatton (27 $^{\circ}$34′S, 152 $^{\circ}$18′E, 94 m asl) on 16 January, 2006 and encountered the highest temperatures. Both expts 1 and 2 were conducted until anthesis, whereas expt 3 was carried through until physiological maturity.

Field experiments were laid out as a randomized complete block design with three replicates and up to seven entries. Only data for 'MR Buster' are considered here. Plot size was four rows of 15 m, with a row spacing of 1 m. Data were collected from well-bordered plants in the centre two rows of each plot, except in cases where poor plant stands required use of well-bordered plants in the outside two rows. Experiments were thinned to a uniform stand of 50 000 plants ha$^{-1}$ before any mutual shading could occur, i.e. around full expansion of the 3rd–4th leaf on the main shoot. Each experiment received a basal fertilizer application prior to sowing and fertilizer and supplemental irrigation were managed to ensure optimum growing conditions throughout the experiments. Atrazine was applied after sowing, but prior to emergence, to control weeds. Insecticides and fungicides were applied as necessary to control heliothis and rust. Minimum, maximum and average air temperature (*T* in $^{\circ}$C with a Campbell Scientific 108-L6; http://www.campbellsci.co.uk/), relative humidity and global solar radiation (Sradn in MJ m$^{-2}$ d$^{-1}$ with a Li-Cor Li200S; http://www.licor.com/) were measured at 1·5 m above the soil surface. Data were recorded hourly using a datalogger (CR10, Campbell Scientific; http://www.campbellsci.com). Radiation interception was measured with two 1 m long tube solarimeters (Type TSL, Delta-T Devices; http://www.delta-t.co.uk/) at ground level in each plot (one tube positioned from row to row and the other from mid-row to mid-row), plus a reference tube outside the crop. Solarimeters were cleaned weekly and dead leaves were removed to ensure that the measured intercepted radiation was due to green leaf area only.

The two controlled environment experiments were carried out in a randomized complete block design with four replicates and six genotypes (including 'MR Buster') in a greenhouse (expt 4) and a phytotron (expt 5) at CIRAD research station in Montpellier, France (43 $^{\circ}$38′N, 3 $^{\circ}$52′E, 46 m asl). The experiments focused on early plant development and were terminated when 8–9 main shoot leaves were fully expanded, around the end of the tiller emergence period. In expt 4, solar radiation was augmented with halogen lamps during cloudy days to

TABLE 1. *Summary of environmental conditions for the five experiments conducted here*

| | Expt 1 | Expt 2 | Expt 3 | Expt 4 | Expt 5 |
|---|---|---|---|---|---|
| Location | Warwick, Australia | Warwick, Australia | Gatton, Australia | Montpellier, France | Montpellier, France |
| Situation | Field | Field | Field | Glasshouse | Phytotron |
| Sowing date | 25 Oct. 2004 | 2 Mar. 2005 | 16 Jan. 2006 | 31 Aug. 2006 | 2 Oct. 2006 |
| Photoperiod at sowing | 13 h 2 min | 12 h 37 min | 13 h 31 min | 13 h 13 min | 13 h 00 min |
| Max. daily radiation ($MJ\ m^{-2}\ d^{-1}$) | 22·9 | 21·0 | 20·3 | 15·0 | 10·0 |
| Average daily min. temperature (°C) | 13·1 | 11·9 | 19·9 | 21·2 | 22·0 |
| Average daily max. temperature (°C) | 27·9 | 30·0 | 33·4 | 38·5 | 28·0 |
| Average daily temperature (°C) | 20·5 | 21·0 | 26·7 | 29·9 | 25·0 |
| Average daily humidity (%) | 58·0 | 60·2 | 65·6 | 63·2 | 70·0 |
| PTQ ($MJ\ m^{-2}\ °Cd^{-1}\ d^{-1}$) [PT] | 2·4 | 2·1 | 1·5 | 0·9 | 0·5 |
| PTQ ($MJ\ m^{-2}\ °Cd^{-1}\ d^{-1}$) [TEM] | 3·3 | 2·6 | 1·3 | 0·5 | 0·7 |
| PTQ ($MJ\ m^{-2}\ °Cd^{-1}\ d^{-1}$) [TSEN] | 1·9 | 2·3 | 1·4 | – | – |
| Cumulative radiation at flag leaf ($MJ\ m^{-2}$) | 1401 | 1241 | 899 | 195* | 245[†] |
| Cumulative thermal time at flag leaf (°Cd) | 604 | 545 | 656 | 310* | 407[†] |

Radiation and temperature values are for the period up to 30 d after sowing (which includes the tiller emergence period). The photo-thermal quotient (PTQ) is calculated for the pre-tillering (PT), tiller emergence (TEM) and tiller senescence (TSEN) periods (see Fig. 1).

\* Values until main shoot L8 is fully expanded.

[†] Values until main shoot L9 is fully expanded.

maintain at least 300 $\mu mol\ m^{-2}\ s^{-1}$ of photosynthetically active radiation (PAR). Radiation was measured with PAR sensors (PAR-IR/M SOLEMS; http:/www.solems.com, measuring the energy of photons for wavelengths between 300 and 700 nm) in $\mu mol\ s^{-1}\ m^{-2}$ and converted into global solar radiation units of $MJ\ m^{-2}\ d^{-1}$ for comparison with field experiments. Temperature was controlled to maintain approximately 20 °C during the night and a cooling system was used when temperature exceeded 35 °C during the day. In expt 5, radiation was provided by halogen lamps at constant intensity. However, mean daily irradiance varied with plant height (closeness to lamps) from 250 (during early growth) to 700 $\mu mol\ m^{-2}\ s^{-1}$ (at last harvest). Daily photoperiod was fixed at 13 h, temperature was set to 28 and 22 °C (day/night) and relative air humidity was between 60 and 80 % (day/night). In both experiments, seeds were germinated for 1 d at 30 °C in an illuminated culture chamber, and subsequently transplanted in drained 1-L pots containing fertilized soil. Pots were watered at least once daily to field capacity with a culture solution (pH 5·5) containing the following nutrients (concentrations in mM): $KH_2PO_4$, 0·21; $K_2HPO_4$, 0·06; $KNO_3$, 1·98; $Ca(NO_3)_2$, 2·96; $MgSO_4$, 0·61; $(NH_4)_2SO_4$, 0·53; $MnSO_4$, $2·9 \times 10^{-3}$; $ZnSO_4$, $2·5 \times 10^{-3}$; KCl, 0·1; $(NH_4)_2MoO_4$, $6 \times 10^{-5}$; $CuSO_4$, $6·3 \times 10^{-2}$; $H_3BO_3$, $7·4 \times 10^{-3}$; EDTA-Fe, 0·206.

### Plant measurements

*Development.* In field experiments, emergence was scored daily on 2 m of row in each plot until complete emergence. Anthesis was scored on five adjacent tagged plants in the inner rows of each plot. Each panicle was rated at least once a week until the beginning of anthesis, and then every 2 d by estimating how far down the panicle anthers were visible. The date of anthesis in each plot was determined when over 50 % of plants had exserted anthers midway down the panicle. Physiological maturity (expt 3 only) was scored on main shoot panicles of ten plants per plot by screening for the presence of a black layer on individual grains. Physiological maturity was reached when 90 % of the panicles had grains that had

reached the black layer stage in the lower part of the panicle (Eastin *et al.*, 1973).

The number of visible, fully expanded and senesced leaves on the main shoot and each tiller was recorded weekly on the five tagged plants per plot in the field and on all plants in the controlled environment experiments. A leaf was visible once its tip was visible above the enclosing leaf whorl, fully expanded once its ligule was visible above the enclosing sheath of the previous leaf and senesced if less than 50 % of its area remained green. Thermal time was calculated from a broken linear function of the hourly mean air temperature, using 11, 30 and 42 °C as the base, optimum and maximum temperatures (Hammer *et al.*, 1993). The average thermal time separating the appearance of successive leaf tips or ligules (tip or ligule phyllochron) was determined as the inverse of the slope of the relationship between leaf number and cumulative thermal time. Leaf expansion duration (LED) was computed for each leaf rank ($L_{rank}$) of the main shoot as the time separating tip and ligule appearance.

*Growth.* In each experiment, the fully expanded area of individual leaf blades was estimated non-destructively from observed blade length and maximum width of each leaf on all axes of the five tagged plants per plot in expts 1–3, and of one plant per replication in expts 4 and 5. Blade length was measured from the ligule to the tip, and blade width at its widest point. Blade area was calculated as the product of length, width and a shape coefficient, which was determined by linear regression of the blade area measured with a leaf area meter (Delta T or LICOR LI-3100C for field experiments; CID CI-203; http://www.cid-inc.com for controlled environment experiments) on the product of leaf length and width of the same leaf. The value of the shape coefficient (0·69) was similar to that reported by McCree *et al.* (1984) and Lafarge *et al.* (2002) for sorghum. However, to calculate plant leaf area during early growth accurately, values of 0·85 and 0·75 were derived from measurements on main shoot L1 and L2, respectively.

Above-ground biomass in field experiments was determined by destructively harvesting an area of $2\,m^2$ (ten plants) at ground level in each plot approximately once a week from thinning to anthesis (expts 1 and 2) or physiological maturity (expt 3). In expts 4 and 5, one plant per replication was harvested at three stages: (1) before any tillers had emerged (before main shoot L4 was fully expanded), (2) after appearance of the first tiller (main shoot L5 or L6 fully expanded) and (3) during tiller appearance (main shoot L8 or L9 fully expanded). Each sample was separated into main shoots and tillers, identified by their rank (see below). For each culm rank, biomass was separated into green leaves, dead leaves, stems (including sheaths) and panicles. Green leaf area was measured with a leaf area meter. Dry weight for each component was obtained after drying at $80\,^{\circ}C$ for at least 7 d. LAI was calculated for each culm from its total green leaf area and the harvested area.

*Tillering characterization.* Tiller emergence was observed weekly on the five tagged plants in each plot, on the plants harvested each week in field experiments and on all individual plants in the controlled environment experiments. The rank of each emerged tiller was defined by the position of the main shoot axillary bud from which it originated, with tiller 1 (T1) emerging from the sheath of main shoot leaf 1. In the present experiments, only primary tillers (developing from main shoot axillary buds) were produced. Tiller appearance was expressed relative to the number of visible or fully expanded main shoot leaves. This resulted in a development index that was not biased by environmental effects on the phyllochron.

Maximum ($N_{\text{tiller,max}}$) and fertile (FTN) tiller number were observed on tagged plants and plants used for destructive sampling. For the tagged plants, the distinction between fertile and arrested/senesced tillers was established for each tiller depending on whether at least one new leaf appeared between successive weekly observations prior to the flag leaf (Lafarge *et al.*, 2002). $N_{\text{tiller,max}}$ included all emerged tillers, irrespective of whether they became fertile or not. FTN in expts 1–3 included only tillers that continued to develop until anthesis and produced a panicle. Tiller rank fertility rate was calculated as the percentage of the total number of emerged tillers for each rank that was fertile.

### Development of a plant *S/D* framework

Data were analysed to seek quantitative associations between tillering and *S/D* indicators. First, PTQ was calculated as a general environmental indicator of *S/D* during the key plant development phases for tillering: (1) pre-tillering, (2) tiller emergence and (3) tiller senescence. The PTQ is a broad-based environmental indicator of available solar radiation per unit of thermal time during a particular period:

$$PTQ = \frac{\sum_{d_1}^{d_2} \frac{I_0}{T_{\text{acc}}}}{d_2 - d_1} \qquad (1)$$

in $MJ\,m^{-2}\,(^{\circ}Cd)^{-1}\,d^{-1}$, where $I_0$ is the incident daily global radiation in $MJ\,m^{-2}\,d^{-1}$, $T_{\text{acc}}$ is daily accumulated thermal time in $(^{\circ}Cd)\,d^{-1}$, and $d_1$ and $d_2$ are the start and end of the considered phase.

Secondly, a form of relative growth rate (RGR, eqn 2), which expresses plant dry weight gain per unit of existing dry weight, but per unit thermal time rather than calendar time, was calculated. In classical growth analysis, RGR is calculated using $W_1$ and $W_2$ at times $t_1$ and $t_2$. The approach adopted here for RGR and relative tillering rate (RTR) follows the method of Hoffmann and Poorter (2002) that uses means of natural log-transformed plant weights rather than the natural logarithm of the mean of plant weights, which can bias RGR estimates if the variance of the natural logarithm transformed weight changes over time:

$$RGR = \frac{[\overline{\ln(W_2)} - \overline{\ln(W_1)}]}{(T_{\text{acc},2} - T_{\text{acc},1})} \qquad (2)$$

RGR in $g\,g^{-1}\,(^{\circ}Cd)^{-1}$, where $W_n$ is plant dry weight on day $n$ and $T_{\text{acc},n}$ is the accumulated thermal time on day $n$. The RGR was compared to the RTR (eqn 3) to check the existence of a robust linear relationship as noted for rice (Dingkuhn *et al.*, 2001):

$$RTR = \frac{[\overline{\ln(N_{\text{tiller},2} + 1)} - \overline{\ln(N_{\text{tiller},1} + 1)}]}{(T_{\text{acc},2} - T_{\text{acc},1})} \qquad (3)$$

RTR in tiller $\text{tiller}^{-1}\,(^{\circ}Cd)^{-1}$, where $N_{\text{tiller},n}$ is the tiller number per plant at $T_{\text{acc},n}$.

Finally, more specific indicators of carbohydrate supply ($S$) and demand ($D$) were calculated to derive a plant-level carbohydrate $S/D_{\text{index}}$ for tillering (eqn 4). Under non-limiting conditions, supply of assimilates to the plant for any specific time period is determined by the amount of radiation intercepted by the plant. At the canopy level, intercepted radiation is commonly calculated as the product of accumulated incident radiation per unit time ($I_0$) and the fraction intercepted by the crop. Once the crop canopy has developed significantly, the fraction of intercepted light can be calculated by comparing light measured with solarimeters placed at ground level in the crop with that found for the reference solarimeter above the crop. However, in the early stages of canopy development (up to full expansion of leaf 5 in this case), sampling via linear solarimeters is not reliable, and we assumed that all leaf area was intercepting light (Lafarge and Hammer, 2002a). Assimilate supply was thus proportional to plant leaf area. However, in order to develop an $S/D_{\text{index}}$ that has the capacity to capture environmental effects on tillering, but is easy to parameterize for large-scale applications, plant leaf area was represented by the final size (Leafsize) of the leaf expanding at the start of tiller emergence. To account for environmental effects on the duration of the developmental period for which assimilate supply was calculated, the size of the leaf used for Leafsize was multiplied by its LED from tip to ligule appearance. The demand for assimilates by the plant can be related to the temperature-driven potential rate of leaf area growth ($\Delta$LA) during the period of tiller appearance, as stem elongation has not commenced at that time (Lafarge and Hammer, 2002a, b). Therefore, a plant-level assimilate $S/D_{\text{index}}$ that extends the PTQ concept and that could be

tested for association with tillering can be represented by the generic formula:

$$S/D_{\text{index}} = (I_0 \times \text{Leafsize} \times \text{LED})/\Delta\text{LA}. \quad (4)$$

## RESULTS

### Environment characterization

The different sowing dates and locations resulted in considerable variation in radiation and temperature across experiments. The PTQ experienced during the pre-tillering and tiller emergence phases (Table 1) was lower in expt 3 than in expts 1 and 2 because of the higher temperature during early development in expt 3. PTQ was lowest in the controlled environment experiments (expts 4 and 5) due to low radiation levels, although high temperature also contributed in expt 4. Field experiments differed significantly in main shoot leaf number, ranging from 13·9 under short days (expt 2) to 17·0 under long days and high temperatures (expt 3), consistent with known responses (Ravi Kumar *et al.*, 2009). This resulted in significant differences in time to full flag leaf expansion.

### Tiller appearance and fertility

Tillering dynamics throughout the crop life cycle were common across all experiments, with a pre-tillering, tiller emergence and tiller senescence phase (Fig. 1A). Tiller emergence commenced between 150 and 170 °Cd in the field experiments, but later in both expt 4 (approx. 200 °Cd) and expt 5 (approx. 250 °Cd). $N_{\text{tiller,max}}$ and FTN varied considerably among experiments (Fig. 1B). $N_{\text{tiller,max}}$ was greatest in expt 2 (4·1) and expt 1 (3·5), followed by expts 4, 3 and 5 (Fig. 1B). $N_{\text{tiller,max}}$ and PTQ were positively but weakly correlated ($R^2 = 0.67$, $P < 0.1$), indicating that PTQ was a useful but limited indicator of potential tillering.

Environmental differences in $N_{\text{tiller,max}}$ were related to the frequency of appearance of early (T1 and T2) and late (T5) tiller ranks. These ranks only appeared with a combined frequency above 1·0 in expts 1, 2 and 4, where $N_{\text{tiller,max}}$ per plant was above 3·0. T3 and T4 always had the highest frequencies compared with other ranks and T3 had a frequency of 1·0 in all experiments except expt 5 (where it was still above 0·8). A consistent hierarchy in tillering, both for emergence and for fertility frequency, was observed for all environments: T3 > [T2,T4] > [T1,T5]. Non-fertile tillers ceased producing new leaves during the tiller senescence phase and then progressively senesced leaves until the end of each experiment.

### Main shoot leaf appearance

The number of visible and fully expanded leaves on the main shoot increased linearly with thermal time (Fig. 2). For the three field experiments, a single linear regression ($R^2 = 0.98$, $n = 15$) fitted data on leaf tip appearance up to flag leaf (Fig. 2), resulting in a tip phyllochron of 27·5 °Cd (± 1·2). Leaf ligule appearance in the field experiments followed a broken linear regression. Prior to the breakpoint, the three field experiments had a common ligule appearance rate, resulting in a ligule phyllochron of 34·5 °Cd (± 0·9). The difference in position of the breakpoint among field experiments was associated with a difference in final leaf number, as the breakpoint occurred around the ligule appearance of the largest leaf, which was three to four leaves before the flag leaf. In the controlled environment experiments, both ligule and tip phyllochrons were significantly longer than in the field (Fig. 2), with tip phyllochrons of 31 °Cd (± 1·5) in expt 4 and 37 °Cd (± 1·4) in expt 5, and ligule phyllochrons of 40 °Cd (± 1·4) in expt 4 and 54 °Cd (± 1·5) in expt 5. As a consequence of the difference between tip and ligule phyllochrons, the LED on each axis increased with leaf rank up to the largest leaf and then decreased rapidly until the flag leaf. The longer LED in controlled environments compared with
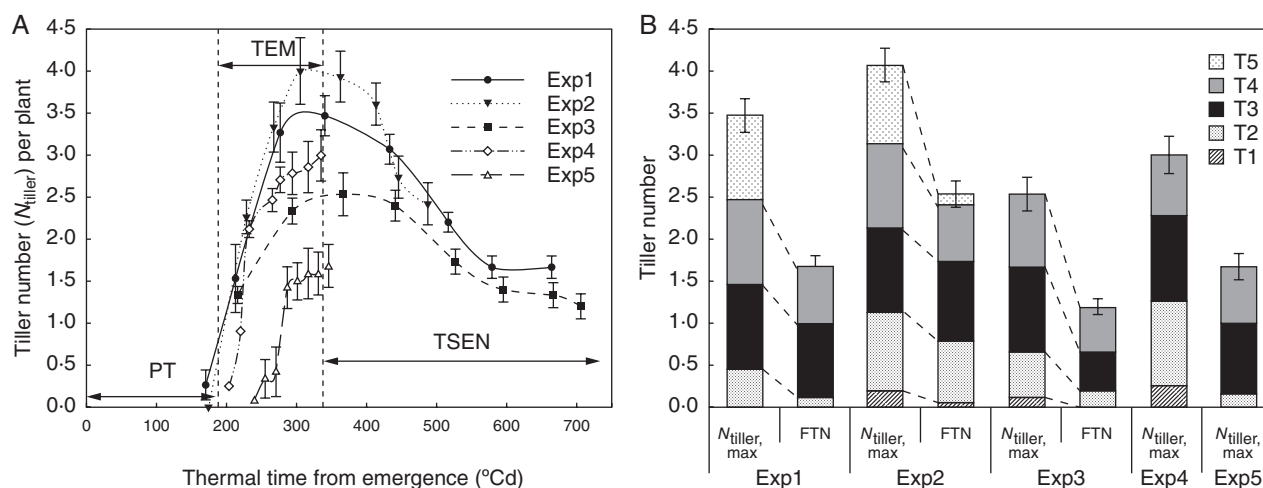


FIG. 1. (A) Tiller number per plant versus thermal time from emergence for the five experiments. PT, pre-tillering period; TEM, tiller emergence period; TSEN, tiller senescence period. Error bars indicate s.e.m. (B) Maximum ($N_{\text{tiller,max}}$) and fertile (FTN) tiller number per plant, including the contribution from each tiller rank ($T_n$) for the five experiments. In controlled environments (expts 4 and 5), only maximum tiller number was observed. Error bars indicate s.e.m.
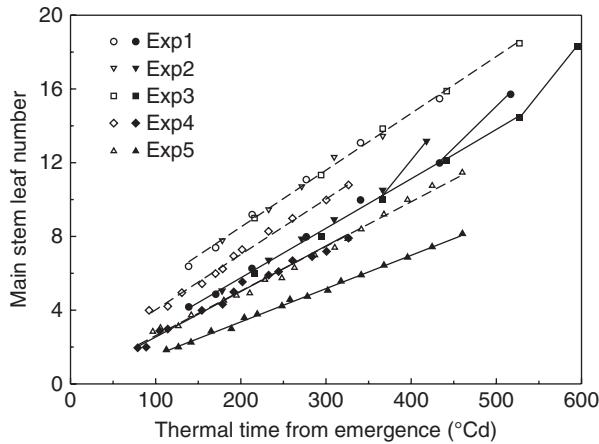
FIG. 2. Main shoot leaf tip (open symbols) and ligule (filled symbols) number versus thermal time in three field experiments (up to flag leaf) and two controlled environment experiments (up to leaf 10). Each data point is the average of 15 tagged plants. There are three regression lines for the number of leaf tips and three for the number of ligules. In each case, the three regressions are for the field experiments (one common regression for data from expts 1–3), expt 4 and expt 5, respectively. The phyllochron is given by the inverse of the regression slope.

field conditions was predominantly due to a slower ligule appearance rate.

### Coordination of main shoot and tiller leaf appearance

Leaf tip and ligule appearance rates for fertile tillers did not differ significantly from those for the main shoot (Fig. 3). In addition, the phenological age (leaf tip number) at which a tiller of a particular rank emerged (represented by the intercept with the *x*-axis of the linear regression of tiller leaf tip number on main shoot leaf tip number) was limited to a narrow phenological window of no more than one tip phyllochron. In field experiments, T2 emerged between main shoot L4 and L5 tip appearance, T3 between main shoot L5 and L6 tip appearance, and T4 between main shoot L6 and L7 tip appearance. In controlled environments, tillers emerged generally one phyllcochron later, with T3 emerging between the tip appearance of main shoot L6 and L7 (Fig. 3). Tiller appearance was therefore highly coordinated with main shoot leaf appearance. Within this context, the late onset of tillering in expt 5 compared with expt 4 (Fig. 1A) was a consequence of the low number of lower-ranked tillers (Fig. 1B). In all experiments, tiller emergence ceased when around 8–9 leaves had fully expanded and crop LAI was approximately 0·5–0·7 (Fig. 4).

Consistent with this coordination between tiller appearance and main shoot leaf appearance, final leaf number per axis declined for successive tillers, such that T4 final leaf number was one less than T3 and two less than T2. This was consistent across all experiments.

### Leaf size profiles

From seedling emergence to the end of the tiller emergence phase, total plant leaf area was predominantly determined by the main shoot (Fig. 4). Significant differences among

experiments in main shoot leaf size were observed from L4 onwards (Fig. 5). Between L4 and L9, which represented the tiller emergence phase, leaves were largest in expt 4, while from L6 onwards, they were smallest in expt 2. Main shoot leaf area profiles of the lower leaves were similar for expts 1 and 3.

Between L4 and the largest leaf, both the length and the width of successive main shoot leaves increased linearly with leaf rank (Fig. 6). The slopes of these relationships, defined here as the leaf length increase rate (LLIR) and leaf width increase rate (LWIR) thus represent the increase in plant leaf area during the tillering period. Environmental differences in leaf size were predominantly due to an effect on leaf length, rather than width (Fig. 6). The relatively high LWIR for expt 4 was probably associated with calcium deficiency, which occurred in response to the high temperatures (Table 1).

### Development of a plant S/D framework

The variability in tillering behaviour across environments (Fig. 1) was associated with variation in crop growth, as RTR (during the time interval between successive biomass samples) increased linearly with RGR during that interval (Fig. 7). This is consistent with the hypothesis that plant carbohydrate availability determines tillering. However, the relationship between RTR and RGR appeared to differ between field and controlled environment experiments, in particular for the intercept. This was probably because RGR does not account for environmental differences in leaf size and LED. Therefore, an indicator of carbohydrate availability that is more specific than RGR is required to better capture the environmental effects on tiller appearance.

The generic $S/D_{index}$ (eqn 4), which quantifies the balance between carbohydrate supply and demand, was adapted for this purpose (eqn 5). At the start of the tiller emergence phase, L5 is expanding on the main shoot (Fig. 3) and environmental effects on leaf size are apparent for L5. The fully expanded area of L5 (LA5) was therefore used to represent environmental effects on Leafsize (eqn 4) and hence plant leaf area at tillering. Additionally, it was anticipated that inclusion of only LA5 could facilitate larger-scale parameterization of eqn (5) compared with including total plant leaf area. The amount of intercepted radiation was calculated from the average incident radiation per unit thermal time for the duration of expansion of main shoot leaf 5 ($RAD_{LED5}$) and the thermal duration of expansion of leaf 5 (LED5). The demand for assimilates was represented by the LLIR, which was the main cause for the environmental differences in leaf size (Fig. 6). LLIR was calculated from L4 to L9, which included the range of leaves that expanded during the tiller emergence phase. As the LLIR was constant between L4 and the longest (largest) leaf, inclusion of L4 did not affect the calculated value of LLIR, but reduced the error in the estimate due to the wider range in leaf number used for the calculation. The $S/D_{index}$ was thus computed as:

$$S/D_{index} = \frac{RAD_{LED5} \times LA5 \times LED5}{LLIR(4-9)} \qquad (5)$$

Across the five experiments, the $S/D_{index}$ was significantly and highly ($R^2 = 0.80$, $P < 0.05$) correlated with $N_{tiller,max}$
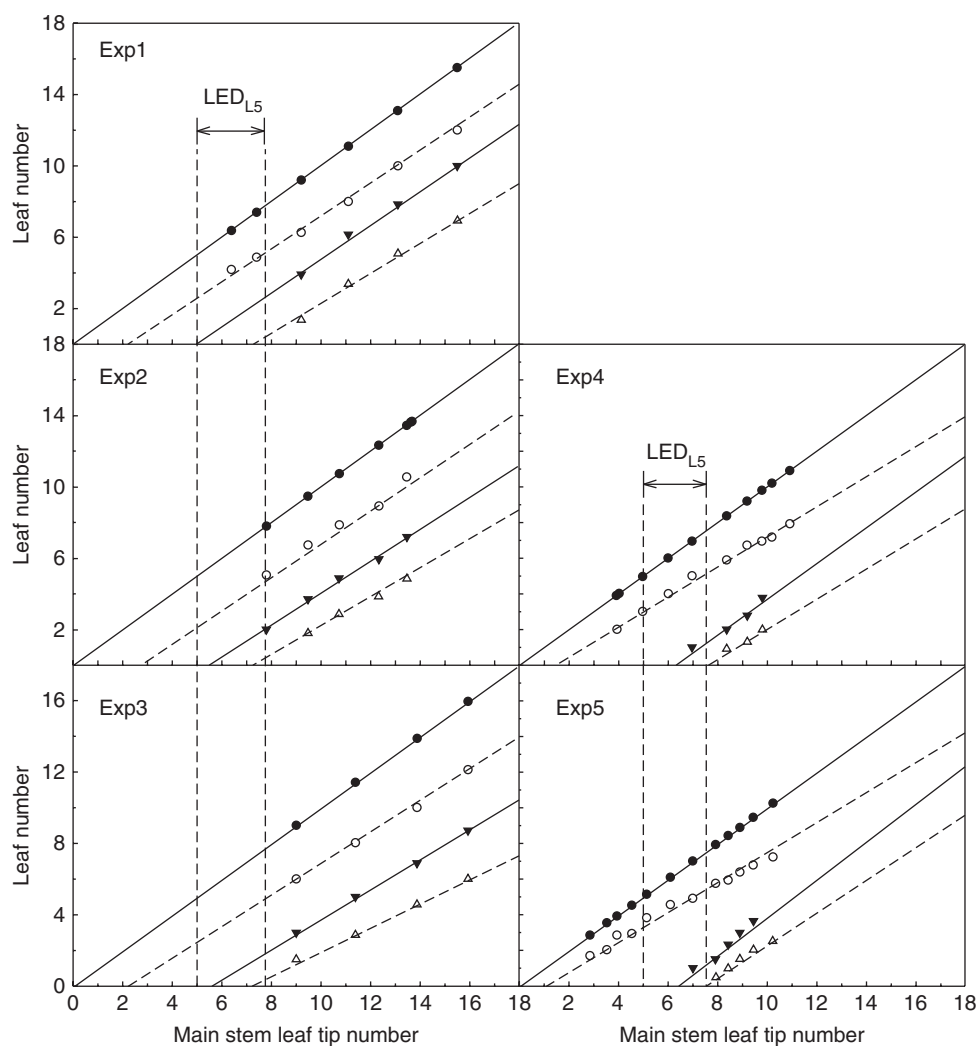
FIG. 3. Number of visible leaves (solid symbols, solid lines) and fully expanded leaves (open symbols, dotted lines) for main shoot (circles) and fertile tiller 3 (triangles) versus the number of visible main shoot leaves. Lines represent linear regressions: $y = a \times x + b$, where $a = 1$ for visible leaves on the main shoot, $0.9 < a < 1.0$ for visible leaves on tiller 3, and $0.7 < a < 0.9$ for fully expanded leaves on the main shoot and tiller 3. Standard errors under 0.2 are not shown. Leaf expansion duration of L5 ($LED_{L5}$) is shown for each experiment.

(Fig. 8). This contrasts with the lesser degree of association found with the more general indicator, PTQ ($R^2 = 0.67$, $P < 0.1$).

## DISCUSSION

In this study, environmental control of tillering in sorghum through regulation of internal plant competition for carbohydrates was quantified by growing a representative hybrid in five experiments with varying radiation and temperature. Results showed that tiller appearance was highly synchronized with main shoot leaf appearance, with a consistent hierarchy for tillering across environments. Environments mainly differed in the frequency of appearance of lower-rank tillers. This explained some of the observed environmental differences in the onset of tiller appearance and was consistent with the hypothesis that internal plant competition determines tillering. A generalized $S/D_{index}$ that accounted for environmental effects on plant development and assimilate supply

and demand explained most of the variation in maximum tiller number observed across experiments.

### Tillering is developmentally regulated

*Coordination of tillering and leaf appearance.* The phenology of main shoots and tillers was highly coordinated. The rate of appearance of successive tillers and the leaf appearance rate of those tillers were similar to the appearance rate of main shoot leaves (Fig. 3). These results were consistent with previous observations on a range of cereals, including sorghum (Lafarge and Hammer, 2002b), pearl millet (Craufurd and Bidinger, 1988; van Oosterom et al., 2001), wheat (Porter, 1985; Rickman et al., 1985) and rice (Tivet et al., 2001). The coordination between main shoot leaf appearance and tiller emergence resulted in each tiller having a window of approximately one phyllochron during which it could appear (Fig. 3). At the meristem level, initiation of cell division and elongation in tiller (*n*) coincides with initiation of cell division in the
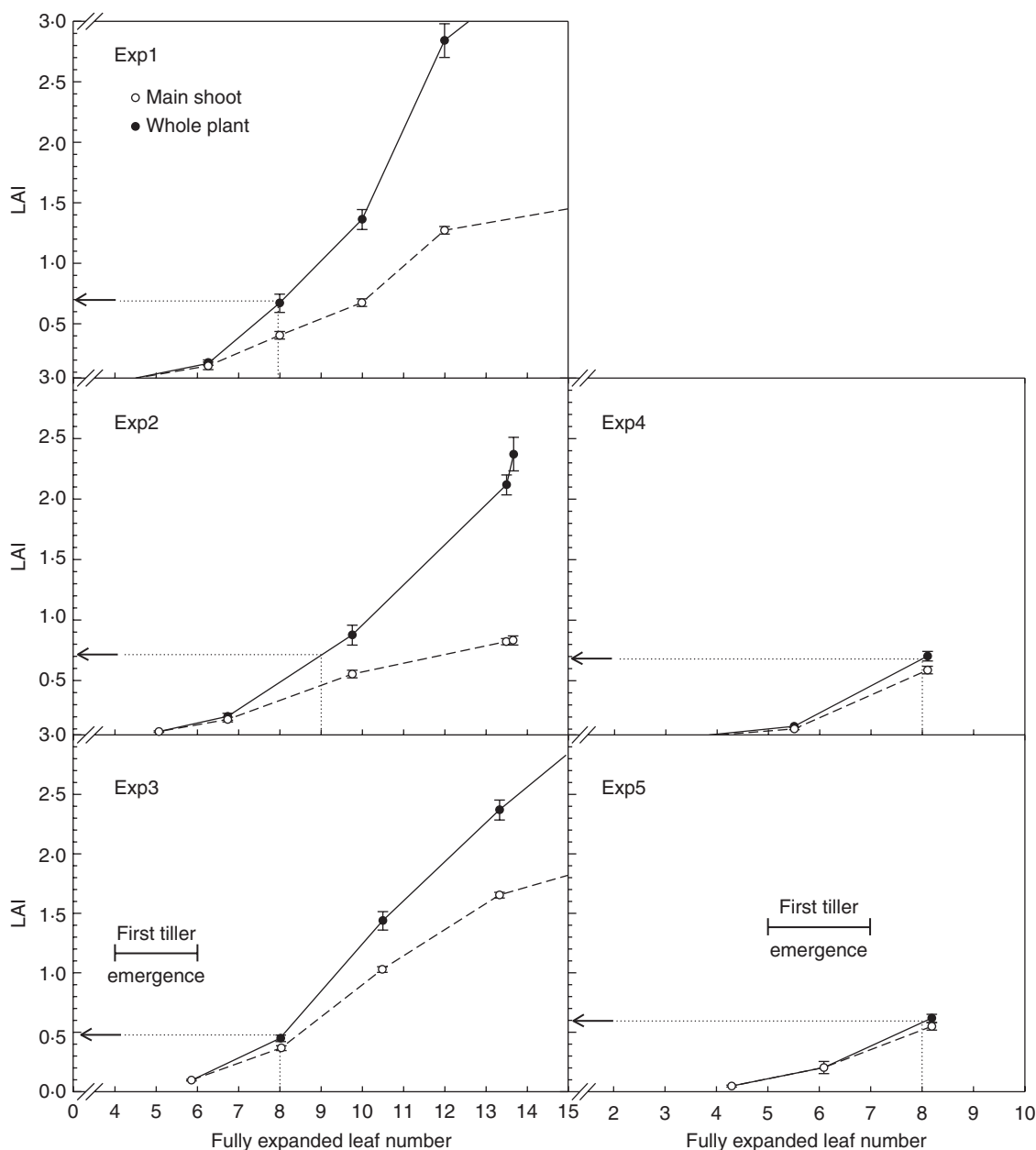
FIG. 4. Leaf area index (LAI) of the main shoot and whole plant, as indicated, during early growth in field (left panels) and controlled environment (right panels) experiments. The timing of the window for first tiller emergence is indicated by a horizontal bar. Horizontal arrows indicate approximate LAI at cessation of tillering. Error bars indicate s.e.m.

primordium of leaf $(n + 2)$ (Skinner and Nelson, 1994). This synchrony was confirmed by the present observation that T3 appeared when the tip of main shoot L5 became visible. Phenological age of the main shoot was thus a robust measure of tillering dynamics, even though the window for tiller appearance was shifted by one leaf rank in controlled environment experiments compared with field experiments. Environmental effects on plant phenology can therefore be important in explaining tillering dynamics in terms of topological location, appearance and fertility frequency.

Cessation of tiller appearance was regulated by main shoot leaf appearance through the crop LAI. The LAI of 0·6–0·7

at which tillering ceased (Fig. 4) was similar to the 0·64 reported for 'MR Buster' across densities (Lafarge and Hammer, 2002*b*). This regulation of tillering cessation by LAI has been linked to signalling of inter-plant competition through the red/far-red ratio of light in the canopy (Casal *et al.*, 1985; Evers *et al.*, 2006).

*Hierarchy in tillering.* The hierarchy across tiller ranks in emergence and fertility frequencies, with T3 > [T2,T4] > [T1,T5], corroborated results of Lafarge *et al.* (2002) for the same hybrid, grown at a range of densities in a single environment. Similarly, the appearance and frequency of fertile tillers in

rice depends on their rank (Jaffuel and Dauzat, 2005). Environments differed predominantly in the frequency of appearance of lower-rank tillers, similar to effects reported for pearl millet (van Oosterom *et al.*, 2001). Because each tiller has a window of around one phyllochron for its appearance, a reduction in the frequency of appearance of lower-rank tillers will delay the onset of tillering as observed in expt 5 (Figs 1 and 3). Within the context of an *S/D* framework, such a delay in the onset of tiller appearance may reflect insufficient assimilate availability for production of lower-rank tillers (Bos and Neuteboom, 1998).

*Regulation of tillering through a* S/D *framework*

Environmental conditions affect tillering through effects on the carbohydrate supply/demand framework. In the absence of drought stress, radiation determines crop growth, whereas temperature drives development. As each tiller has only one phyllochron during which it can appear, temperature determines the duration of this period. Consequently, low radiation and high temperature limit carbohydrate availability at the start of the tiller emergence period, resulting in a low frequency of appearance of early tillers. Although this explains the positive



FIG. 5. Individual size of fully expanded main shoot leaves versus leaf rank for the five experiments.

effect of PTQ on tiller appearance, PTQ does not consider the extent of radiation interception (supply) or environmental effects on assimilate demand via plant growth. This limitation was illustrated by the findings in expt 4, where $N_{tiller,max}$ per plant was close to that observed in expt 3 (Fig. 1), despite a much lower PTQ (Table 1). To better account for the environmental control of tillering through regulation of the carbohydrate supply/demand balance, an $S/D_{index}$ (eqn 5) was developed that also accounted for environmental effects on tillering through plant growth. This increased the variation in tillering explained across experiments and the statistical significance of the association from 67 % ($P < 0.1$) for PTQ to 80 % ($P < 0.05$) for the $S/D_{index}$. Hence, in addition to improved biological sensibility, the $S/D_{index}$ provided a more significant and robust association with environmental effects on tillering.

The environment affected leaf area dynamics of the main shoot during tillering through effects on leaf length and phyllochron. An environmental effect on leaf length, rather than width, has been reported for sorghum (Kaitaniemi *et al.*, 1999; Lafarge and Tardieu, 2002) and maize (Reymond *et al.*, 2004) and was due to changes in the leaf elongation rate in response to temperature, vapour pressure deficit and water availability. In the present experiments, leaf length in expts 2 and 3 was similar to that observed for the same sorghum hybrid by Lafarge and Hammer (2002*b*) in field experiments. The longer leaves and longer phyllochron in controlled environments were probably a consequence of growth responses to the low light intensity, which may have limited assimilate availability for leaf expansion or invoked shade plant responses (Smith and Whitelam, 1997). Similar effects of radiation levels on leaf length and phyllochron have been observed for maize (Birch *et al.*, 1998; Muller *et al.*, 2001). Environmental effects on plant growth and development thus affect both the supply and the demand term of the $S/D_{index}$ (eqn 5) through an effect on LED and LLIR, respectively.

The effect of the $S/D_{index}$ on plant growth could account for the tillering hierarchy of lower-rank tillers. As plant leaf area expands, intercepted radiation increases, causing an increase in assimilate supply. Because assimilate demand (LLIR) is more conservative over time, $S/D_{index}$ gradually increases over time. Because the appearance frequency of a tiller rank
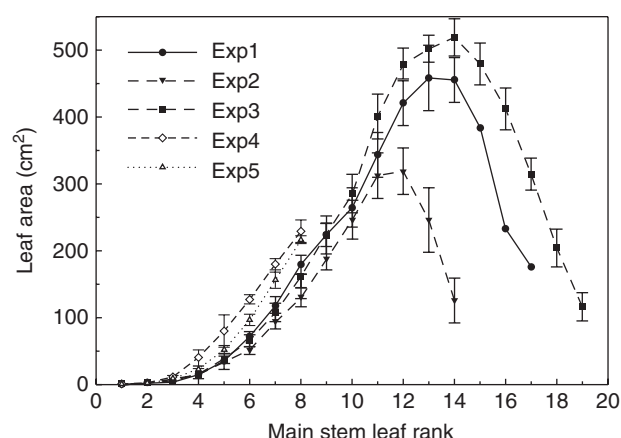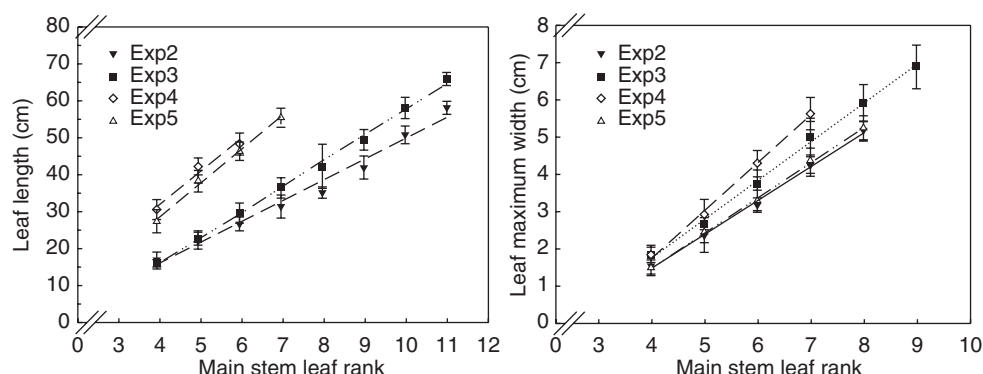


FIG. 6. Length and width of main shoot leaves versus leaf rank in field (expts 2 and 3) and controlled environment experiments (expts 4 and 5). Regression slopes for length are 5·6 (±0·2), 6·8 (±0·2), 9·8 (±0·5) and 9·3 (±0·5) for expts 2–5, respectively. Regression slopes for width are 0·9 (±0·1), 1·0 (±0·1), 1·3 (±0·1) and 0·9 (±0·1) for expts 2–5, respectively. Error bars indicate s.e.m.
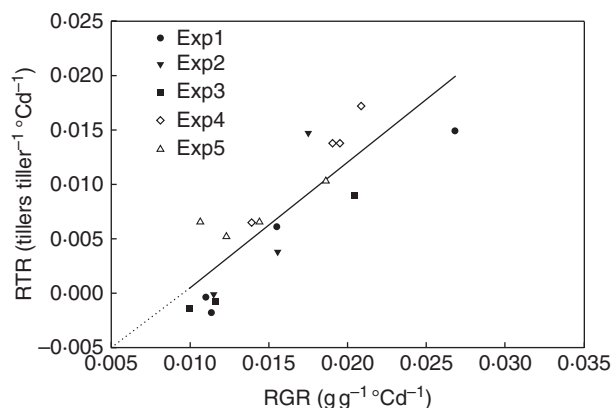
FIG. 7. Relative tillering rate (RTR) versus relative growth rate (RGR) from tiller emergence to tiller cessation for field experiments (closed symbols) and controlled environment experiments (open symbols). Individual data points represent the RGR and RTR between two successive biomass samples. Common linear regression: RTR = $1.15$ ($\pm 0.03$) $\times$ RGR $- 0.011$ ($\pm 0.002$), $R^2 = 0.72$, $P < 0.05$.
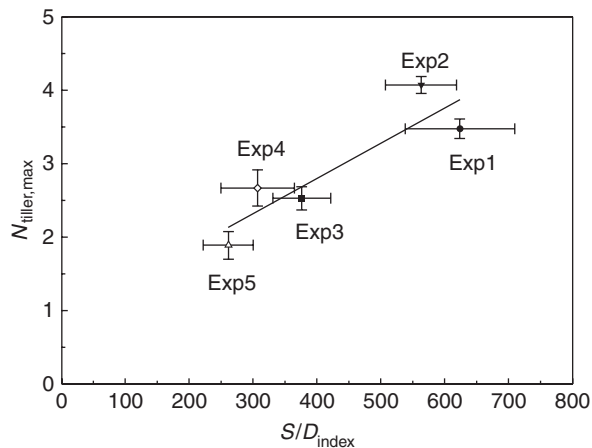


FIG. 8. Response of maximum tiller number ($N_{tiller,max}$) per plant to $S/D_{index}$ for all five experiments. For calculation of $S/D_{index}$, see text. Regression equation: $N_{tiller,max} = 0.0048 \times S/D_{index} + 0.89$, $R^2 = 0.80$, $P < 0.05$. Error bars indicate s.e.m.

is a function of the $S/D$ balance during the period it could emerge, this temporal evolution of the $S/D_{index}$ could explain the high frequency of appearance of T3 and T4 as a consequence of the $S/D$ balance being consistently above the threshold required to initiate a tiller only once L5 was elongating. However, it does not capture the decline in appearance frequency of high-rank tillers, as this was more probably linked to signalling of inter-plant competition through light quality (Casal *et al.*, 1985). It has been suggested that this competition effect via light quality also accounts for the reduced emergence of high-rank tillers at greater plant density, as the effect would be invoked earlier at higher density (Lafarge and Hammer, 2002*b*).

The $S/D_{index}$ provided a unifying framework that could explain the environmental effects on tillering across the diverse experiments conducted (Fig. 8). In the field experiments, differences in leaf size were small (Fig. 5) and the low $N_{tiller,max}$ per plant in expt 3 was predominantly due to

high temperatures (Table 1), which hastened development and reduced intercepted radiation during expansion of L5, causing a decline in the $S/D_{index}$ (eqn 5). For controlled environments, the similar $N_{tiller,max}$ per plant in expt 4 compared with expt 3 (Fig. 1), despite a much lower PTQ (Table 1), could be explained by the large area of L5 (Fig. 5) and the long phyllochron (Fig. 2), which caused an increase in supply (eqn 5). This more than compensated for the increased demand associated with the high LLIR (Fig. 6), resulting in a similar $S/D_{index}$ in expts 4 and 3 (Fig. 8). The low $N_{tiller,max}$ per plant in expt 5 was due to the failure of lower rank tillers to emerge because of the low PTQ during the pre-tillering phase (Table 1). The results support the hypothesis that a simple $S/D_{index}$ can explain much of the observed variability in tillering, at least for this particular cultivar. Its ability to account for environmental effects on plant growth provides a biological functionality that is lacking in the PTQ approach. This gives the $S/D_{index}$ a robustness and predictive value that could provide the basis for dynamic simulation of tillering in crop growth models. The applicability of this framework for tillering responses across a range of germplasm is tested in an associated study (Kim *et al.*, 2010).

## LITERATURE CITED

**Birch CJ, Vos J, Kiniry J, Bos HJ, Elings A. 1998.** Phyllochron responds to acclimation to temperature and irradiance in maize. *Field Crops Research* **59**: 187–200.

**Bos HJ, Neuteboom JH. 1998.** Morphological analysis of leaf and tiller number dynamics of wheat (*Triticum aestivum* L.): responses to temperature and light intensity. *Annals of Botany* **81**: 131–139.

**Casal JJ, Sanchez RA, Deregibus VA. 1985.** Variations in tiller dynamics and morphology in *Lolium multiflorum* Lam. vegetative and reproductive plants as affected by differences in red/far-red irradiation. *Annals of Botany* **56**: 553–559.

**Casal JJ, Sanchez A, Deregibus VA. 1986.** The effect of plant density on tillering: the involvement of R/FR ratio and the proportion of radiation intercepted per plant. *Environmental and Experimental Botany* **26**: 365–371.

**Choudhury BJ. 2001.** Modeling radiation- and carbon-use efficiencies of maize, sorghum, and rice. *Agricultural and Forest Meteorology* **106**: 317–330.

**Conway G, Toenniessen G. 1999.** Feeding the world in the twenty-first century. *Nature* **402**: C55–C58.

**Craufurd PQ, Bidinger FR. 1988.** Effect of duration of the vegetative phase on shoot growth, development and yield in pearl millet (*Pennisetum americanum* (L.) Leeke). *Journal of Experimental Botany* **39**: 124–139.

**Davies A, Thomas H. 1983.** Rates of leaf and tiller production in young spaced perennial ryegrass plants in relation to soil temperature and solar radiation. *Annals of Botany* **57**: 591–597.

**Deregibus VA, Sanchez A, Casal JJ, Trlica MJ. 1985.** Tillering responses to enrichment of red light beneath the canopy in a humid natural grassland. *Journal of Applied Ecology* **22**: 199–206.

**Dingkuhn M, Tivet F, Siband P, Asch F, Audebert A, Sow A. 2001.** Varietal differences in specific leaf area: a common physiological determinant of

tillering ability and early growth vigor? In: Peng S, Hardy B. eds. *Rice research for food security and poverty alleviation*. Los Banos, Philippines: International Rice Research Institute, 95–108.

**Dingkuhn M, Luquet D, Kim HK, Tambour L, Clement-Vidal A. 2006.** Ecomeristem, a model of morphogenesis and competition among sinks in rice: 2. Simulating genotype responses to phosphorus deficiency. *Functional Plant Biology* **33**: 325–337.

**Eastin JD, Hultquist JH, Sullivan CY. 1973.** Physiologic maturity in grain sorghum. *Crop Science* **13**: 175–178.

**Evers JB, Vos J, Andrieu B, Struik PC. 2006.** Cessation of tillering in spring wheat in relation to light interception and red : far-red ratio. *Annals of Botany* **97**: 649–658.

**Fischer KS, Wilson GL. 1975.** Studies of grain production in *Sorghum bicolor* (L. Moench). V. Effect of planting density on growth and yield. *Australian Journal of Agricultural Research* **26**: 31–41.

**Friend DJC. 1965.** Tillering and leaf production in wheat as affected by temperature and light intensity. *Canadian Journal of Botany* **43**: 1063–1076.

**Hammer GL, Muchow RC. 1994.** Assessing climatic risk to sorghum production in water-limited subtropical environments. I. Development and testing of a simulation model. *Field Crops Research* **36**: 221–234.

**Hammer GL, Hill K, Schrodter G. 1987.** Leaf area production and senescence of diverse grain sorghum hybrids. *Field Crops Research* **17**: 305–317.

**Hammer GL, Carberry PS, Muchow RC. 1993.** Modelling genotypic and environmental control of leaf area dynamics in grain sorghum. I. Whole plant level. *Field Crops Research* **33**: 293–310.

**Heiniger RW, Vanderlip RL, Welch SM. 1997.** Developing guidelines for replanting grain sorghum: I. Validation and sensitivity analysis of the SORKAM sorghum growth model. *Agronomy Journal* **89**: 75–92.

**Hoffmann WA, Poorter H. 2002.** Avoiding bias in calculations of relative growth rate. *Annals of Botany* **90**: 37–42.

**Honda T, Okajima H. 1970.** Environmental light conditions and tiller development in the rice plant. 3. Effects of partial shading and temperature on the development of tiller buds and dry matter increments. *Bulletin of the Institute for Agricultural Research* **22**: 1–15.

**Jaffuel S, Dauzat J. 2005.** Synchronism of leaf and tiller emergence relative to position and to main stem development stage in a rice cultivar. *Annals of Botany* **95**: 401–412.

**Johnson IR, Riha SJ, Wilks DS. 1995.** Modelling daily net canopy photosynthesis and its adaptation to irradiance and atmospheric $CO_2$ concentration. *Agricultural Systems* **50**: 1–35.

**Kaitaniemi P, Room PM, Hanan JS. 1999.** Architecture and morphogenesis of grain sorghum, *Sorghum bicolor* (L.) Moench. *Field Crops Research* **61**: 51–60.

**Katayama T. 1951.** *Studies on tillering of rice, wheat and barley.* Tokyo: Yokendo.

**Khush GS. 1999.** Green revolution: preparing for the 21st century. *Genome* **42**: 646–655.

**Kim HK, Luquet D, van Oosterom EJ, Dingkuhn M, Hammer GL. 2010.** Regulation of tillering in sorghum: genotypic effects. *Annals of Botany* **106**: 69–78.

**Kirby EJM, Faris DG. 1972.** The effect of plant density on tiller growth and morphology in barley. *Journal of Agricultural Science* **78**: 281–288.

**Kirby EJM, Appleyard M, Fellowes G. 1985.** Leaf emergence and tillering in barley and wheat. *Agronomie* **5**: 193–200.

**Lafarge TA, Hammer GL. 2002a.** Predicting plant leaf area production: shoot assimilate accumulation and partitioning, and leaf area ratio, are stable for a wide range of sorghum population densities. *Field Crops Research* **77**: 137–151.

**Lafarge TA, Hammer GL. 2002b.** Tillering in grain sorghum over a wide range of population densities: modelling dynamics of tiller fertility. *Annals of Botany* **90**: 99–110.

**Lafarge T, Tardieu F. 2002.** A model co-ordinating the elongation of all leaves of a sorghum cultivar was applied to both Mediterranean and Sahelian conditions. *Journal of Experimental Botany* **53**: 715–725.

**Lafarge TA, Broad IJ, Hammer GL. 2002.** Tillering in grain sorghum over a wide range of population densities: identification of a common hierarchy

for tiller emergence, leaf area development and fertility. *Annals of Botany* **90**: 87–98.

**Li X, Qian Q, Fu Z, *et al*. 2003.** Control of tillering in rice. *Nature* **422**: 618–621.

**Luquet D, Dingkuhn M, Kim HK, Tambour L, Clement-Vidal A. 2006.** EcoMeristem, a model of morphogenesis and competition among sinks in rice. 1. Concept, validation and sensitivity analysis. *Functional Plant Biology* **33**: 309–323.

**Mazzella MA, Bertero D, Casal JJ. 2000.** Temperature-dependent internode elongation in vegetative plants of *Arabidopsis thaliana* lacking phytochrome B and crytochrome 1. *Planta* **210**: 497–501.

**McCree KJ, Kallsen CE, Richardson SG. 1984.** Carbon balance of sorghum plants during osmotic adjustment to water stress. *Plant Physiology* **76**: 898–902.

**Muller B, Reymond M, Tardieu F. 2001.** The elongation rate at the base of a maize leaf shows an invariant pattern during both the steady-state elongation and the establishment of the elongation zone. *Journal of Experimental Botany* **52**: 1259–1268.

**Neuteboom JH, Lantinga EA. 1989.** Tillering potential and relationship between leaf and tiller production in perennial ryegrass. *Annals of Botany* **63**: 265–279.

**Nix HA. 1976.** Climate and crop productivity in Australia. In: Yoshida S. ed. *Climate and crop*. Los Banos, Philippines: IRRI, 495–507.

**Ong CK, Marshall C. 1979.** The growth and survival of severely-shaded tillers in *Lolium perenne* L. *Annals of Botany* **43**: 147–155.

**van Oosterom EJ, Carberry PS, Hargreaves JNG, O'Leary GJ. 2001.** Simulating growth, development, and yield of tillering pearl millet II. Simulation of canopy development. *Field Crops Research* **72**: 67–91.

**van Oosterom E, Hammer G, Kim HK, McLean G, Deifel K. 2008.** Plant design features that improve grain yield of cereals under drought. In: Unkovich M. ed. *Global Issues, Paddock Action. Proceedings of the 14th Australian Society of Agronomy Conference*. CD ROM. Gosford, Australia: The Regional Institute, www.agronomy.org.au.

**Ortiz-Monasterio JI, Dhillon SS, Fischer RA. 1994.** Date of sowing effects on grain yield and yield components of irrigated spring wheat cultivars and relationships with radiation and temperature in Ludhiana, India. *Field Crops Research* **37**: 169–184.

**Porter JR. 1985.** Approaches to modelling canopy development in wheat. In: Day W, Akins RK. eds. *Wheat growth modelling*. New York: Plenum Press, 69–81.

**Ravi Kumar S, Hammer GL, Broad I, Harland P, McLean G. 2009.** Modelling environmental effects on phenology and canopy development of diverse sorghum genotypes. *Field Crops Research* **111**: 157–165.

**Reymond M, Muller B, Tardieu F. 2004.** Dealing with the genotype × environment interaction via a modelling approach: a comparison of QTLs of maize leaf length or width with QTLs of model parameters. *Journal of Experimental Botany* **55**: 2461–2472.

**Rickman RW, Klepper B, Peterson CM. 1985.** Wheat seedling growth and development response to incident photosynthetically active radiation. *Agronomy Journal* **77**: 283–287.

**Rosenthal WD, Vanderlip RL, Jackson BS, Arkin GF. 1989.** *SORKAM: A sorghum crop growth model*. College Station, TX: Texas Agricultural Station, TAES Computer Software Documentation Series MP1669.

**Skinner RH, Nelson CJ. 1994.** Epidermal cell division and the coordination of leaf and tiller development. *Annals of Botany* **74**: 9–15.

**Smith H, Whitelam GC. 1997.** The shade avoidance syndrome: multiple responses mediated by multiple phytochromes. *Plant Cell and Environment* **20**: 840–844.

**Tardieu F, Granier C, Muller B. 1999.** Modelling leaf expansion in a fluctuating environment: are changes in specific leaf area a consequence of changes in expansion rate? *New Phytologist* **143**: 33–43.

**Tivet F, da Silveira Pinheiro B, de Raissac M, Dingkuhn M. 2001.** Leaf blade dimensions of rice (*Oryza sativa* and *Oryza glaberrima* Steud.). Relationships between tillers and main stem. *Annals of Botany* **88**: 507–511.